

# STRUCTURAL AND REACTIVITY INSIGHTS INTO SULFATED $\alpha$ -1 LINKED LIGNIN DERIVATIVES: A DFT-BASED COMPARATIVE ANALYSIS

UTKIRJON HOLIKULOV,\* FERIDE AKMAN,\*\* BEKZOD KHUDAYKULOV,\*  
ALEKSANDR S. KAZACHENKO\*\*\*,\*\*\*\*,\*\*\*\*\* and YURIY N. MALYAR<sup>D,E</sup>

\**Department of Optics and Spectroscopy, Samarkand State University,  
15 University Blvd., 140104, Samarkand, Uzbekistan*

\*\**Vocational School of Food, Agriculture and Livestock, University of Bingöl, Bingöl 12000, Turkey*

\*\*\**Reshetnev Siberian State University of Science and Technology, Institute of Chemical Technologies,  
Prospekt Mira 82, Krasnoyarsk, Russia*

\*\*\*\**Siberian Federal University, Pr. Svobodny 79, Krasnoyarsk, 660041 Russia*

\*\*\*\*\**Institute of Chemistry and Chemical Technology, Krasnoyarsk Science Center, Siberian Branch,  
Russian Academy of Sciences, Akademgorodok 50/24, Krasnoyarsk, 660036 Russia*

\*\*\*\*\**Prof. V.F. Voino-Yasenetsky Krasnoyarsk State Medical University of the Ministry of Healthcare  
of the Russian Federation, Str. Partizan Zheleznnyak, Bld. 1, Krasnoyarsk, 660022, Russia*

*Received August 10, 2025*

This work aims to study the structure, charge distribution, and vibrational characteristics of  $\alpha$ -1 lignin and  $\alpha$ -1 lignin sulfate molecules based on density functional theory (DFT) at the B3LYP/6-31G(d,p) level of theory. The addition of a sulfur group to the  $\alpha$ -1 molecule resulted in the formation of the  $\alpha$ -1 lignin sulfate molecule, and the geometry of the O-H bond changed. Based on the APT (Atomic Polar Tensor) and Mulliken charge distribution, the charge of the  $\alpha$ -1 lignin sulfate molecule was significantly different from that of  $\alpha$ -1 lignin, indicating that it had a larger polarization, which was important in intermolecular interactions. In addition, the molecular electrostatic potential (MEP) map showed that the  $\alpha$ -1 lignin sulfate molecule has a large number of nucleophilic and electrophilic sites that are active in hydrogen (H)-bonding. The  $\alpha$ -1 molecule is highly reactive, as indicated by the small HOMO-LUMO energy gap. Based on the global reactivity properties, the  $\alpha$ -1 molecule is more nucleophilic than  $\alpha$ -1 lignin sulfate, which indicates its chemical stability. The presence of vibrations of the O-H, C-H, N-H, C=C, and S-O functional groups in these molecules was theoretically calculated, which was in agreement with the experimental results (scaled at 0.9608). In general, the  $\alpha$ -1 lignin sulfate molecule has strong polarizability, structure, and reactivity, which may be used in materials science and biological sensors in the future.

**Keywords:** lignin, lignin model compounds, sulfated lignin, DFT

## INTRODUCTION

Lignin is one of the most common natural aromatic polymers, comprising up to 30% of the dry weight of wood and playing a key role in the formation of the structure of plant cell walls.<sup>1</sup> The chemical structure of lignin is characterized by a complex three-dimensional architecture formed by the polymerization of oxidized forms of coniferyl, sinapyl and p-coumaric alcohols, which leads to the formation of a branched network consisting of phenylpropane structural units.<sup>2</sup> These units are linked to each other by various types of bonds, including ether ( $\beta$ -O-4,  $\alpha$ -1, 4-O-5) and carbon-carbon ( $\beta$ -5,  $\beta$ - $\beta$ , 5-5) bonds, which determines the high chemical stability and complexity of processing this biopolymer.<sup>3</sup> Despite the abundance of lignin in nature and its potential as a renewable source of aromatic compounds, its industrial use is limited due to its high molecular weight, heterogeneity of structure and limited solubility in most organic solvents.<sup>4</sup> In this regard, considerable attention is paid to the development of methods for modifying lignin aimed at improving its physicochemical properties and expanding the scope of application.

One of the most promising approaches is sulfation – the process of introducing sulfo groups ( $-\text{SO}_3\text{H}$ ) into the lignin molecule, which significantly changes its hydrophilic, surface and ion-exchange properties.<sup>5</sup> Sulfated derivatives of lignin are widely used in various industries. In the construction industry, they are used as plasticizers for concrete mixtures, improving fluidity and reducing the water-cement ratio.<sup>6</sup> In the petrochemical industry, lignosulfonates are used as additives for well drilling,

improving the rheological properties of drilling fluids.<sup>6</sup> In the medical and pharmaceutical industries, sulfated lignins demonstrate antiviral activity, antioxidant properties, and the ability to form complexes with metals.<sup>7</sup> In addition, they are used in the production of biodegradable polymers, heavy metal sorbents, and as stabilizers for various dispersed systems.<sup>6,8</sup> However, the study of the structure of natural lignin and its modified forms is complicated by its high molecular heterogeneity and the complexity of analytical characteristics. To overcome these difficulties, model compounds, which are low-molecular analogues of lignin structural fragments, are widely used in scientific research.<sup>9</sup> Such compounds allow a detailed study of the mechanisms of chemical reactions, the determination of the reactivity of various functional groups, and the establishment of patterns in the change in properties upon modification of the molecule.<sup>10</sup> The key model compounds of lignin are phenolic derivatives containing various substituents in the benzene ring and alkyl chain. Among the most common models, guaiacol, syringol, vanillin, coniferyl alcohol, and their derivatives can be distinguished.<sup>11</sup> These compounds reproduce the main structural elements of lignin and allow studying the influence of various functional groups on the properties of the molecule.

In recent decades, quantum chemical methods have become an integral part of research in the field of chemistry of natural compounds and their modifications.<sup>12</sup> Density functional theory (DFT) methods allow calculating with high accuracy the geometric parameters of molecules, the energies of molecular orbitals, the distribution of electron density and the thermodynamic characteristics of reactions.<sup>13</sup> These methods are especially effective in the study of aromatic systems, where it is important to take into account the effects of conjugation and delocalization of electrons.<sup>14</sup>

Quantum chemical calculations allow not only interpreting experimental data, but also predicting new properties of compounds, optimizing synthesis conditions and developing new materials with specified characteristics. In particular, when studying sulfated derivatives of lignin, DFT methods allow evaluating the influence of sulfo groups on the electronic structure of the molecule, determining changes in the geometry of the molecule after modification and calculating the activation energies of key reaction stages.<sup>15,16</sup> Research conducted in this area shows that the introduction of sulfonic groups into the lignin molecule leads to significant changes in its electronic structure. The sulfonic group, as a strong electron-withdrawing substituent, affects the distribution of electron density in the aromatic ring, which can change the reactivity of other functional groups in the molecule.<sup>17</sup>

A distinction should be made between two processes: sulfonation, which is the introduction of a sulfo group  $-\text{SO}_3\text{H}$  through a C–S bond, which is typical of technical lignosulfonates obtained during sulfite pulping; and sulfation, which is the formation of an ester bond  $\text{C}-\text{O}-\text{S}(=\text{O})_2-\text{OH}$ , when a sulfate group is added to the hydroxyl groups of lignin. In this work, we study sulfation, since it allows the introduction of sulfate groups into the residual OH groups of lignin without destroying the aromatic skeleton and is of interest for the production of biocompatible materials with anticoagulant and antioxidant properties.<sup>18,19</sup>

Quantum-chemical modeling of model lignin compounds and their sulfated derivatives is an important tool for understanding the molecular mechanisms of lignin modification and predicting the properties of the resulting materials. The data obtained can be used to optimize the processes of obtaining functional materials based on lignin and the development of new biocompatible compounds with desired properties. The dimer, linked via an  $\alpha$ -1 bond, was chosen as a model fragment and plays an important role in the formation of stable carbon-carbon bonds in the biopolymer.<sup>9</sup> The primary aim of this work has been to provide a detailed quantum-chemical understanding of how O-sulfation modifies the structural, electronic, and vibrational properties of an  $\alpha$ -1-linked lignin dimer – a representative carbon-carbon bonded model compound of softwood lignin. Using density functional theory (DFT) at the B3LYP/6-31G(d,p) level, we investigate the changes in optimized geometry, atomic charge distributions (APT and Mulliken), molecular electrostatic potential (MEP), frontier molecular orbitals (HOMO-LUMO), global reactivity descriptors, and vibrational (IR) spectra upon introduction of a sulfate group ( $-\text{OSO}_3\text{H}$ ).

## EXPERIMENTAL

### Computational details

Some electronic properties of  $\alpha$ -1 lignin and  $\alpha$ -1 lignin sulfate were modeled using the Gaussian 09W,<sup>20</sup> and GaussView 5.0<sup>21</sup> graphical interfaces. Throughout the work, the DFT method and the Becke 3–Lee–Yang–Parr (B3LYP)/6-31G(d,p) functional set were used to calculate the optimal geometry, frequency, and other molecular

properties.<sup>22,23</sup> The resulting vibrational frequencies were scaled by a factor of 0.9608 to account for anharmonicity and systematic basis error. All calculations were performed in the gas phase without taking solvation into account, as intramolecular substitution effects are being investigated.

## RESULTS AND DISCUSSION

### Optimized geometry

Table 1 shows the geometric parameters of  $\alpha$ -1 lignin and its sulfated derivative obtained in the calculations; bond lengths (Å) and bond angles (°). In both molecules, the structure of the aromatic ring is preserved unchanged (Fig. 1), which indicates the stability of the structure.<sup>24</sup> The introduction of  $-\text{SO}_3\text{H}\text{NH}_3$  into the  $\alpha$ -1 lignin molecule and the formation of  $\alpha$ -1 lignin sulfate lead to significant changes in the O-H bonds. The length of both O-H bonds in  $\alpha$ -1 lignin is 0.9661 Å, and the O-H bond length in  $\alpha$ -1 lignin sulfate increased to 1.0572 Å as a result of the addition of  $-\text{SO}_3\text{H}\text{NH}_3$ . Also, while  $\alpha$ -1 lignin has two O-H hydrogen bond formation zones, the  $\alpha$ -1 lignin sulfate molecule contains newly formed hydrogen bonds (S=O and N-H), which can enhance intermolecular interactions. The changes in angles also indicate that the arrangement of these groups directly affects the shape of the molecule.

Table 1  
Calculated bond lengths and angles for a)  $\alpha$ -1 lignin and b)  $\alpha$ -1 lignin sulfate

	a		b
Bond lengths (Å)			
C1-C2	1.3961	C1-C2	1.3961
C1-C6	1.3969	C1-C6	1.3968
C1-H16	1.0883	C1-H21	1.0882
C2-C3	1.4002	C2-C3	1.4004
C2-O15	1.3684	C2-O18	1.3679
C3-C4	1.3897	C3-C4	1.3896
C3-H17	1.0851	C3-H22	1.0849
C4-C5	1.4041	C4-C5	1.4044
C4-H18	1.0868	C4-H23	1.0867
C5-C6	1.3972	C5-C6	1.3972
C5-C7	1.5198	C5-C7	1.5185
C6-H19	1.0873	C6-H24	1.0872
C7-C8	1.5198	C7-C8	1.521
C7-H20	1.0977	C7-H25	1.0974
C7-H21	1.0977	C7-H26	1.0979
C8-C9	1.3972	C8-C9	1.4001
C8-C13	1.4041	C8-C13	1.4025
C9-C10	1.3969	C9-C10	1.3952
C9-H22	1.0873	C9-H27	1.0869
C10-C11	1.396	C10-C11	1.3903
C10-H23	1.0883	C10-H28	1.0841
C11-C12	1.4002	C11-C12	1.3939
C11-O14	1.3684	C11-O14	1.4049
C12-C13	1.3897	C12-C13	1.3926
C12-H24	1.0851	C12-H29	1.084
C13-H25	1.0868	C13-H30	1.0861
O14-H26	0.9661	O14-S15	1.6597
O15-H27	0.9661	S15-O16	1.4499
		S15-O17	1.466
		S15-O19	1.5676
		O18-H31	0.9661
		O19-H35	1.0572
		N20-H32	1.0167
		N20-H33	1.0166
		N20-H34	1.0195
		N20-H35	1.5398
Bond angles (°)			
C2-C1-C6	119.7981	C2-C1-C6	119.7874

C2-C1-H16	120.1043	C2-C1-H21	120.1222
C6-C1-H16	120.0975	C6-C1-H21	120.0903
C1-C2-C3	119.6257	C1-C2-C3	119.6475
C1-C2-O15	122.9335	C1-C2-O18	122.9304
C3-C2-O15	117.4408	C3-C2-O18	117.422
C2-C3-C4	119.7907	C2-C3-C4	119.8021
C2-C3-H17	118.8789	C2-C3-H22	118.9028
C4-C3-H17	121.3303	C4-C3-H22	121.295
C3-C4-C5	121.5608	C3-C4-C5	121.5034
C3-C4-H18	119.1401	C3-C4-H23	119.115
C5-C4-H18	119.2974	C5-C4-H23	119.3804
C4-C5-C6	117.7436	C4-C5-C6	117.806
C4-C5-C7	121.0163	C4-C5-C7	120.9864
C6-C5-C7	121.2331	C6-C5-C7	121.201
C1-C6-C5	121.4804	C1-C6-C5	121.453
C1-C6-H19	118.988	C1-C6-H24	118.9822
C5-C6-H19	119.5313	C5-C6-H24	119.5643
C5-C7-C8	114.866	C5-C7-C8	115.1051
C5-C7-H20	109.4792	C5-C7-H25	109.6473
C5-C7-H21	108.4568	C5-C7-H26	108.5742
C8-C7-H20	108.4563	C8-C7-H25	108.4005
C8-C7-H21	109.4801	C8-C7-H26	109.0201
H20-C7-H21	105.7118	H25-C7-H26	105.6786
C7-C8-C9	121.2362	C7-C8-C9	120.6649
C7-C8-C13	121.013	C7-C8-C13	120.9364
C9-C8-C13	117.7439	C9-C8-C13	118.383
C8-C9-C10	121.4804	C8-C9-C10	121.2802
C8-C9-H22	119.531	C8-C9-H27	119.4873
C10-C9-H22	118.9883	C10-C9-H27	119.2325
C9-C10-C11	119.7981	C9-C10-C11	118.8982
C9-C10-H23	120.0975	C9-C10-H28	121.5903
C11-C10-H23	120.1044	C11-C10-H28	119.5105
C10-C11-C12	119.626	C10-C11-C12	121.2783
C10-C11-O14	122.9343	C10-C11-O14	118.8081
C12-C11-O14	117.4396	C12-C11-O14	119.8282
C11-C12-C13	119.7904	C11-C12-C13	119.0231
C11-C12-H24	118.8782	C11-C12-H29	119.5366
C13-C12-H24	121.3314	C13-C12-H29	121.439
C8-C13-C12	121.5606	C8-C13-C12	121.1345
C8-C13-H25	119.2958	C8-C13-H30	119.4116
C12-C13-H25	119.1421	C12-C13-H30	119.4527
C11-O14-H26	108.9575	C11-O14-S15	116.4998
C2-O15-H27	108.9571	O14-S15-O16	108.6797
		O14-S15-O17	107.8193
		O14-S15-O19	97.1877
		O16-S15-O17	120.1331
		O16-S15-O19	110.6048
		O17-S15-O19	109.9097
		C2-O18-H31	109.0136
		S15-O19-H35	109.8098
		H32-N20-H33	108.1389
		H32-N20-H34	108.3602
		H32-N20-H35	115.0476
		H33-N20-H34	108.4302
		H33-N20-H35	116.1582
		H34-N20-H35	100.0388

---

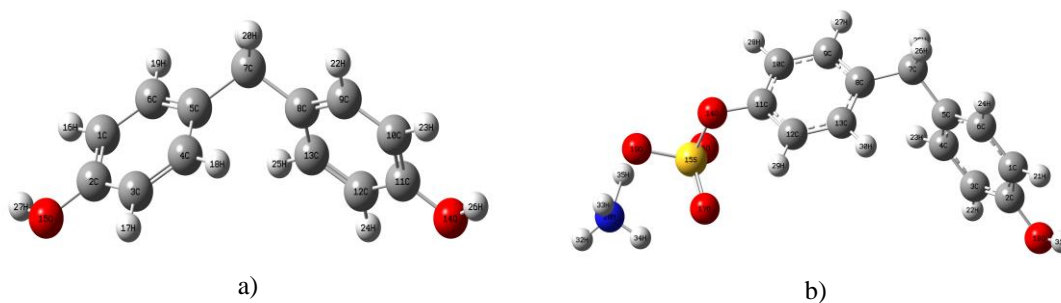


Figure 1: Optimized molecular structures of a)  $\alpha$ -1 lignin and b)  $\alpha$ -1 lignin sulfate

Some significant geometric changes are observed in the  $\alpha$ -1 lignin sulfate modification. In particular, there are the following major changes in the bond angles: substitution of  $-\text{COOH}$  with  $-\text{SO}_3\text{H}$  led to an increase in the angles by up to  $8^\circ$ . In particular, the O-S-O angles resemble tetrahedral geometry. The addition of the  $\text{SO}_3\text{H}$  group makes the molecule more flexible, which may also affect the reactivity. When looking at the angles in the aromatic rings, there was almost no change.

### APT charge vs Mulliken charge analysis

The electron density distribution in molecules is important in explaining the reactivity, polarization and spectroscopic properties of molecules.<sup>25</sup> In this work, the APT (Atomic Polar Tensor) and Mulliken charges were calculated for  $\alpha$ -1 lignin and  $\alpha$ -1 lignin sulfate molecules and their results were compared and analyzed (Fig. 2, Table 2). Knowing the APT charge distribution is especially useful in studies with IR spectra and dipole moments, and provides information about the behavior of the molecule in an electric field.<sup>26</sup> The Mulliken charge distribution, on the other hand, provides the basis for the orbital-based electron density.

According to the APT approach, the 2C and 11C atoms of the  $\alpha$ -1 lignin molecule have a high positive charge (about +0.58 e), which indicates a low electron density in these atoms. The 14O and 15O atoms, on the contrary, have a negative charge (about -0.75 e), and the electron density is more concentrated due to the high electronegativity of oxygen. Although the Mulliken charge distribution is also much lower than the APT charge, their direction (positive or negative) is similar for most atoms. The difference in charges in the  $\alpha$ -1 lignin sulfate molecule is significantly larger than that of  $\alpha$ -1 lignin. The APT charge of the 15S atom has a high positive charge (about +2.47 e), indicating the presence of a small electron density around it. The 19O atom has a negative charge (-1.15 e), which indicates a high degree of polarization. This means that the  $\alpha$ -1 lignin sulfate molecule has a high electrical polarization.

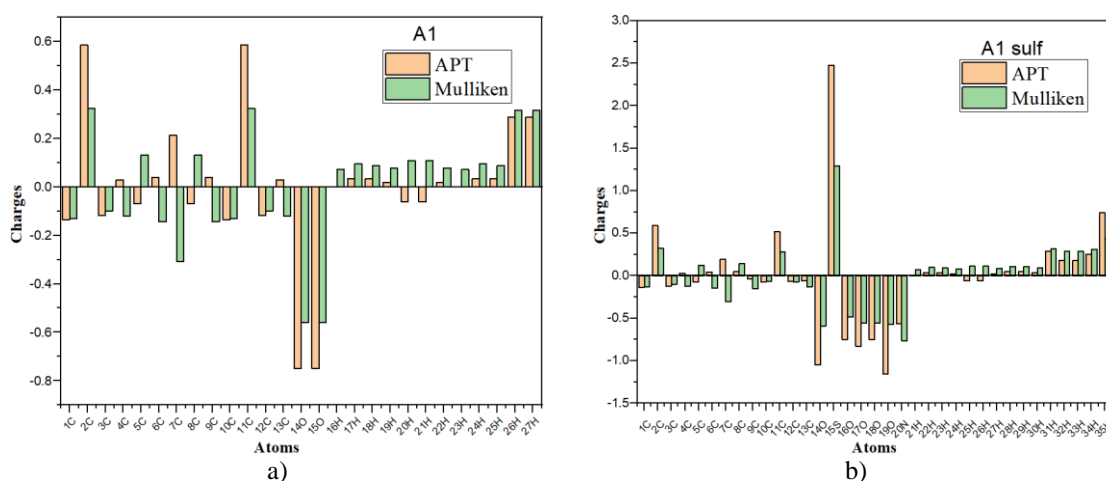


Figure 2: APT and Mulliken charge distributions for a)  $\alpha$ -1 lignin and b)  $\alpha$ -1 lignin sulfate

Table 2  
APT and Mulliken charges for a)  $\alpha$ -1 lignin and b)  $\alpha$ -1 lignin sulfate

a			b		
Atoms	APT charges	Mulliken charges	Atoms	APT charges	Mulliken charges
1C	-0.13465	-0.12977	1C	-0.13566	-0.13011
2C	0.58477	0.32271	2C	0.59057	0.32349
3C	-0.11718	-0.09936	3C	-0.12093	-0.09935
4C	0.02893	-0.12089	4C	0.03144	-0.12077
5C	-0.07016	0.13065	5C	-0.07334	0.12377
6C	0.03973	-0.14381	6C	0.04336	-0.14296
7C	0.21205	-0.30818	7C	0.19366	-0.30675
8C	-0.07014	0.13063	8C	0.04692	0.14196
9C	0.03973	-0.14381	9C	-0.03631	-0.15177
10C	-0.13466	-0.12977	10C	-0.07225	-0.06805
11C	0.58477	0.32271	11C	0.51751	0.27752
12C	-0.11717	-0.09935	12C	-0.0675	-0.07257
13C	0.02896	-0.12088	13C	-0.06038	-0.1293
14O	-0.74987	-0.56014	14O	-1.04616	-0.59171
15O	-0.74988	-0.56014	15S	2.47656	1.29147
16H	0.0013	0.07126	16O	-0.75075	-0.48439
17H	0.0333	0.09414	17O	-0.82737	-0.55297
18H	0.03404	0.08755	18O	-0.75019	-0.55899
19H	0.01909	0.07847	19O	-1.15594	-0.57354
20H	-0.06218	0.10769	20N	-0.5653	-0.76862
21H	-0.06215	0.10768	21H	0.00176	0.07175
22H	0.01909	0.07847	22H	0.03672	0.09768
23H	0.00131	0.07126	23H	0.03548	0.09386
24H	0.0333	0.09414	24H	0.01966	0.0788
25H	0.03403	0.08754	25H	-0.05981	0.11205
26H	0.28681	0.31561	26H	-0.0611	0.11286
27H	0.28682	0.31561	27H	0.01831	0.08538
			28H	0.05056	0.1098
			29H	0.04986	0.10534
			30H	0.0352	0.09365
			31H	0.28736	0.3158
			32H	0.17937	0.28603
			33H	0.1778	0.28535
			34H	0.25126	0.31173
			35H	0.73962	0.43356

### MEP and ESP analyses

Molecular electrostatic potential (MEP) and electrostatic surface potential (ESP) maps, which on the electron density surfaces, indicate the electron distribution and the parts of reaction or interaction in the molecule.<sup>27</sup>

According to Figure 3, the regions depicted in red and yellow within the MEP maps of  $\alpha$ -1 lignin and  $\alpha$ -1 lignin sulfate correspond to areas characterized by high electron density and negative electrostatic potential, which typically exhibit susceptibility to electrophilic attack. Conversely, the blue regions indicate areas of positive electrostatic potential, suggesting potential sites for interaction with nucleophilic species.<sup>28</sup>

For the  $\alpha$ -1 lignin molecule, the negative potential is observed around the oxygen atoms O14, O15 in the hydroxyl group, which can form H-bonds through these sites. The ESP contour map shows that the charges are symmetrically distributed around the molecule, which indicates the delocalization (stability) of the electron density of the aromatic ring.<sup>29</sup> The electron density distribution is quite polar due to the SO<sub>3</sub>H group in the  $\alpha$ -1 lignin sulfate molecule. The red dots on the O16, O17, and O19 atoms surrounding the S15 atom indicate that they have a deep negative potential. This means that the molecule is more likely to be electrostatically engaged (H-bonding or dipole-dipole interaction). According to the

ESP contour surfaces, the charges in the  $\alpha$ -1 lignin sulfate molecule are unevenly distributed, which indicates that this molecule has a higher reactivity and stronger molecular interactions in polar solutions.

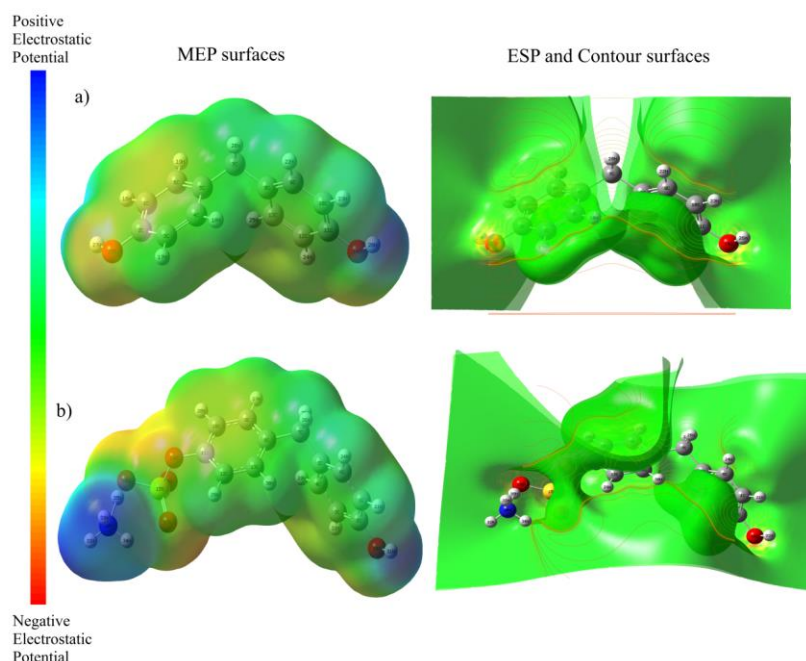


Figure 3: MEP (left) and ESP (right) surface maps of a)  $\alpha$ -1 lignin and b)  $\alpha$ -1 lignin sulfate

### Frontier orbital and global reactivity analyses

According to molecular orbital theory, the reactivity of molecules depends on their HOMO (Highest Occupied Molecular Orbital) and LUMO (Lowest Unoccupied Molecular Orbital).<sup>30</sup> HOMO and LUMO represent the electron-donating and electron-accepting properties of a molecule, respectively, and the energy gap ( $\Delta E$ ) between them is a parameter that determines the stability and reactivity of the molecule, that is the smaller gaps typically correlate with higher reactivity and lower kinetic stability.<sup>31</sup> Figure 4 shows the distribution of HOMO and LUMO orbitals of  $\alpha$ -1 lignin (a) and  $\alpha$ -1 lignin sulfate (b) molecules. The electron densities in HOMO orbitals are mainly located in aromatic ring or functional groups. In  $\alpha$ -1 linked lignin and sulfated  $\alpha$ -1 linked lignin molecules, HOMO orbitals are mostly centered in the aromatic system and  $-\text{OH}$  group, while LUMO orbitals extend only in the aromatic region in  $\alpha$ -1 lignin and more in the aromatic ring and sulfonic group in the  $\alpha$ -1 lignin sulfate molecule. This situation can alter the molecule's reactivity and its ability to gain or lose electrons.<sup>32</sup> According to the results, the  $\Delta E$  of the  $\alpha$ -1 linked lignin molecule (5.5685 eV) is slightly smaller than that of the  $\alpha$ -1 linked lignin sulfate (5.6085 eV). A smaller  $\Delta E$  indicates that the molecule is more sensitive to external influences, and here the  $\alpha$ -1 lignin molecule has a slightly higher reactivity, which is important for photophysical or electrophilic/nucleophilic reactions. The global reactivity and chemical behavior of the molecules are evaluated using the parameters shown in Table 3. The stability against ionization is related to the ionization potential (IP), which is higher for the  $\alpha$ -1 linked lignin sulfate molecule.

Similarly, the electron affinity (EA) (also  $\Delta N_{\text{max}}$ , maximum electron transfer ability) and electrophilicity ( $\omega$ ) are also higher for  $\alpha$ -1 lignin sulfate, which means that it is more electron accepting and more efficient in reactions with electron donating molecules. The nucleophilicity (N) is higher in the  $\alpha$ -1 lignin molecule, which means that it is a greater electron donating molecule. In general, the A1 molecule has a higher nucleophilicity and a smaller  $\Delta E$ , which is useful in chemical synthesis and photophysical processes, as well as high reactivity. The  $\alpha$ -1 lignin sulfate molecule, on the other hand, has higher stability, electrophilicity, and electron acceptor properties.

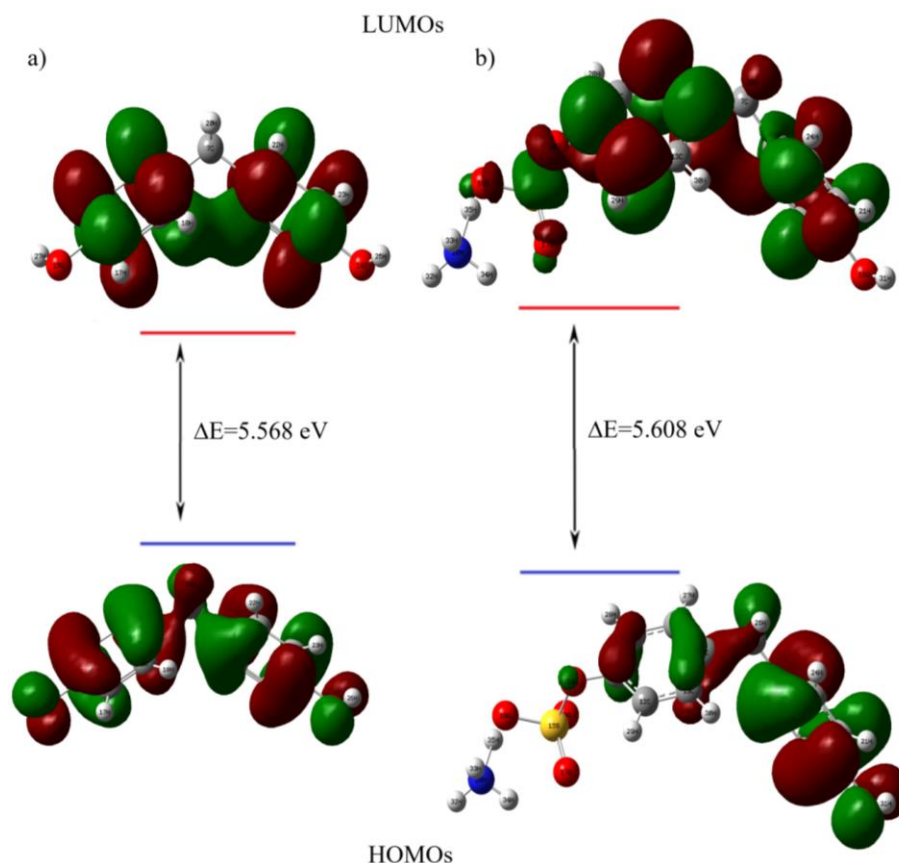


Figure 4: HOMO-LUMO energy diagrams of a)  $\alpha$ -1 lignin and b)  $\alpha$ -1 lignin sulfate, calculated at the B3LYP/6-31G(d,p) level of theory

Table 3

HOMO and LUMO energies, energy band gap, ionization potential, electron affinity, electronegativity, chemical potential, chemical hardness and softness, global electrophilicity index, maximum charge transfer index, optical softness and nucleophilicity index for a)  $\alpha$ -1 linked lignin and b)  $\alpha$ -1 linked lignin sulfate, respectively

Molecule	<b>a</b>	<b>b</b>
$E_{\text{HOMO}}$	-5.6461	-5.7996
$E_{\text{LUMO}}$	-0.0776	-0.1910
$E_g$	5.5685	5.6085
IP	5.6461	5.7996
EA	0.0776	0.1910
$\chi$	2.8618	2.9953
$\mu$	-2.8618	-2.9953
$\eta$	2.7843	2.8043
$\zeta$	0.3592	0.3566
$\omega$	1.4708	1.5997
$\Delta N_{\text{max}}$	1.0279	1.0681
$\sigma_o$	0.1796	0.1783
$N$	0.6799	0.6251

### Vibrational (IR) spectral analysis

In analyzing the structural and functional groups of molecules, it is important to determine their vibrational properties.<sup>33</sup> Figure 5 shows the theoretical FT-IR spectra calculated at the B3LYP/6-31G(d,p) level for the  $\alpha$ -1 lignin and  $\alpha$ -1 lignin sulfate molecules, with the calculated frequencies adjusted using a scalar factor of 0.9608 (Table 4).

In the FT-IR spectrum of the  $\alpha$ -1 lignin molecule, strong vibrations at  $3673 \text{ cm}^{-1}$  correspond to the  $\nu$  O-H stretching vibration.<sup>34</sup> The ranges  $3084\text{--}3036 \text{ cm}^{-1}$  and  $2940\text{--}2906 \text{ cm}^{-1}$  correspond to aromatic and aliphatic C-H stretching vibrations, respectively.<sup>35</sup> The range  $1610\text{--}1497 \text{ cm}^{-1}$  corresponds to C=C

stretching vibrations, while the bending ( $\delta$ ) vibrations characteristic of the  $\text{CH}_2$  group are located between  $1435$  and  $1432\text{ cm}^{-1}$ .<sup>36,37</sup> When the  $\alpha$ -1 lignin sulfate molecule is considered, the  $\nu\text{O-H}$  stretching vibration is observed at  $3672\text{ cm}^{-1}$ , while broad vibrations associated with the  $\text{N-H}$  group are observed at frequencies of  $3476$ – $3335\text{ cm}^{-1}$  and  $2184$ ,  $1620$ ,  $1610$ ,  $1474\text{ cm}^{-1}$ , suggesting the formation of hydrogen bonds. The ranges of  $3098$ – $3038\text{ cm}^{-1}$  and  $2941$ – $2908\text{ cm}^{-1}$  correspond to aromatic and aliphatic  $\text{C-H}$  stretching vibrations, respectively. The frequencies corresponding to the vibrations of the  $\text{S-O}$  group are as follows:  $1286$ ,  $1097$ ,  $879$  and  $704\text{ cm}^{-1}$ . Although the IR spectra for the  $\alpha$ -1 linked lignin and  $\alpha$ -1 linked lignin sulfate molecules generally have similar vibrational regions, the  $\alpha$ -1 lignin sulfate molecule has a more complex molecular structure and contains additional  $\text{S-O}$  stretching and  $\text{N-H}$  groups with a broad vibrational region, which imply a greater capacity for hydrogen bonding.

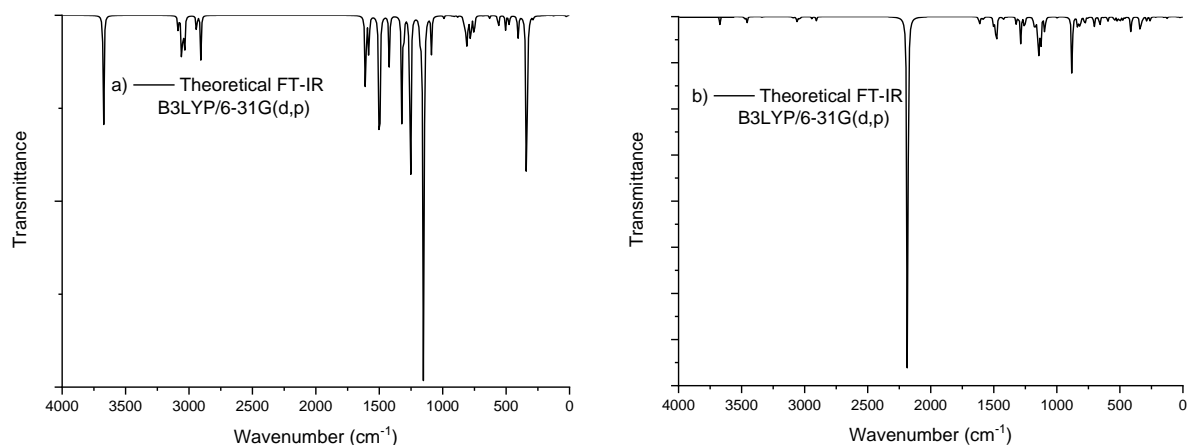


Figure 5: Theoretical FT-IR spectra of a)  $\alpha$ -1 lignin and b)  $\alpha$ -1 lignin sulfate

Table 4  
Selected important theoretical (scaled by a factor of 0.9608) and experimental vibrational frequencies ( $\text{cm}^{-1}$ ) for a)  $\alpha$ -1 lignin and b)  $\alpha$ -1 lignin sulfate

Assignments	a		Assignments	b	
	Theor.	Exp. <sup>15</sup>		Theor.	Exp. <sup>15</sup>
$\nu\text{O-H}$	3673	3400-3600	$\nu\text{O-H}$	3672	3400-3600
$\nu\text{C-H}$ (aromatic)	3084-3036	2950-2900	$\nu, \delta\text{N-H}$	3476-3335, 2184, 1620, 1610, 1474	3450-3300
$\nu\text{C-H}$ (aliphatic)	2940-2906		$\nu\text{C-H}$ (aromatic)	3098-3038	2950-2900
$\nu\text{C=C}$	1610-1497	1600-1500	$\nu\text{C-H}$ (aliphatic)	2941-2908	
$\delta\text{CH}_2$	1435	1440	$\nu\text{C=C}$	1609-1485	1600-1500
			$\delta\text{CH}_2$	1432	1444
			$\nu\text{S-O}$	1286, 1097, 879, 704	1250-1245

## CONCLUSION

In this study, the quantum-chemical analysis of  $\alpha$ -1 lignin and  $\alpha$ -1 lignin sulfate molecules was carried out using the DFT method. According to the optimal geometry, it was found that the  $\alpha$ -1 lignin sulfate molecule underwent more structural changes through changes in the  $\text{O-H}$  bond length. APT and Mulliken charge analyses showed that the  $\alpha$ -1 lignin sulfate molecule has a more polarized electronic structure. MEP and ESP maps showed that  $\alpha$ -1 linked lignin sulfate contains more reactive regions and stronger electrophilic sites compared to  $\alpha$ -1 linked lignin. It was revealed from HOMO-LUMO analyses that the  $\alpha$ -1 lignin sulfate molecule has higher electrophilicity index and kinetic stability and that the  $\Delta E_g$  in the  $\alpha$ -1 lignin molecule is slightly smaller. FT-IR spectral analysis also revealed that there was a difference in the vibrations of the two molecules. Due to the  $\text{S-O}$  and  $\text{N-H}$  bonds in the  $\alpha$ -1 lignin sulfate molecule, the molecule has a greater tendency to  $\text{H-bond}$  and represents the complexity of the molecule. These analyses, together with the establishment of a reliable theoretical basis for further study of these molecules, demonstrate that the  $\alpha$ -1 lignin sulfate molecule demonstrates enhanced stability,

electrostatic potential, and electron-accepting properties, making it a promising candidate for biological activity and chemical sensors.

While this DFT study does not replace experimental characterization (such as gel permeation chromatography or <sup>31</sup>P-NMR spectroscopy), it provides valuable molecular descriptors (atomic charges, electrophilicity, hardness) that can be correlated with macroscopic properties. The obtained results provide theoretical guidance for interpreting the experimental spectra and for selecting the most promising sulfation sites.

**ACKNOWLEDGMENTS:** The authors thank the University of Bingöl for the server and the University of Bitlis Eren for the Gaussian 09W software. This study was carried out within the budget project FWES-2026-0011 for the Institute of Chemistry and Chemical Technology, Siberian Branch of the Russian Academy of Sciences.

## REFERENCES

- <sup>1</sup> J. Zakzeski, P. C. A. Bruijninx, A. L. Jongerius and B. M. Weckhuysen, *Chem. Rev.*, **110**, 3552 (2010), <https://doi.org/10.1021/cr900354u>
- <sup>2</sup> C. G. Boeriu, D. Bravo, R. J. A. Gosselink and J. E. G. Dam, *Ind. Crop. Prod.*, **20**, 205 (2004)
- <sup>3</sup> A. Sand and J. Tuteja (Eds.), “Lignin - Chemistry, Structure, and Application”, IntechOpen, 2023, <https://doi.org/10.5772/intechopen.102263>
- <sup>4</sup> A. Vishtal and A. Kraslawski, *BioResources*, **6**, 3547 (2011)
- <sup>5</sup> Yu. N. Malyar, A. S. Kazachenko, N. Yu. Vasilyeva, O. Yu. Fetisova, V. S. Borovkova *et al.*, *Catal. Today*, **399**, 397 (2022), <https://doi.org/10.1016/j.cattod.2021.07.033>
- <sup>6</sup> T. Tang, J. Fei, Y. Zheng, J. Xu, H. He *et al.*, *ChemistrySelect*, **8**, e202204941 (2023), <https://doi.org/10.1002/slct.202204941>
- <sup>7</sup> T. Aro and P. Fatehi, *ChemSusChem*, **10**, 1861 (2017)
- <sup>8</sup> J. Ruwoldt, “Emulsion Stabilization with Lignosulfonates”, IntechOpen, 2023, <https://doi.org/10.5772/intechopen.107336>
- <sup>9</sup> C. W. Lahive, P. C. J. Kamer, C. S. Lancefield and P. J. Deuss, *ChemSusChem*, **13**, 4238 (2020)
- <sup>10</sup> L. Yang, K. Seshan and Y. Li, *Catal. Today*, **298**, 276 (2017), <https://doi.org/10.1016/j.cattod.2016.11.030>
- <sup>11</sup> O. P. Taran, A. V. Miroshnikova, S. V. Baryshnikov, A. S. Kazachenko, A. M. Skripnikov *et al.*, *Catalysts*, **12**, 1384 (2022), <https://doi.org/10.3390/catal12111384>
- <sup>12</sup> K. P. Zois and D. Tzeli, *Atoms*, **12**, 65 (2024), <https://doi.org/10.3390/atoms12120065>
- <sup>13</sup> A. S. Kazachenko, F. Akman, N. Y. Vasilieva, N. Issaoui, Y. N. Malyar *et al.*, *Int. J. Mol. Sci.*, **23**, 1602 (2022), <https://doi.org/10.3390/ijms23031602>
- <sup>14</sup> V. Mehmeti and M. Sadiku, *Computation*, **10**, 68 (2022), <https://doi.org/10.3390/computation10050068>
- <sup>15</sup> A. S. Kazachenko, F. Akman, N. Y. Vasilieva, Y. N. Malyar, O. Y. Fetisova *et al.*, *Polymers*, **14**, 3000 (2022), <https://doi.org/10.3390/polym14153000>
- <sup>16</sup> F. Akman, A. S. Kazachenko and Y. Malyar, *Cellulose Chem. Technol.*, **55**, 41 (2021), <https://doi.org/10.35812/CelluloseChemTechnol.2021.55.05>
- <sup>17</sup> A. S. Kazachenko, F. Akman, U. Holikulov, A. Jumabaev and Yu. N. Malyar, *Mendeleev Commun.*, **36**, 260 (2026), <https://doi.org/10.71267/mencom.7910>
- <sup>18</sup> M. H. Paulson, *J. Am. Oil Chem. Soc.*, **29**, 556 (1952), <https://doi.org/10.1007/BF02632651>
- <sup>19</sup> G. Dado and R. Bernhardt, in “Kirk Othmer Encyclopedia of Chemical Technology”, John Wiley and Sons, 2017, <https://doi.org/10.1002/0471238961.1921120611140107.a01.pub3>
- <sup>20</sup> M. J. Frisch, G. W. Trucks, H. B. Schlegel, G. E. Scuseria, M. A. Robb *et al.*, Gaussian 09, Revision D.1, Gaussian, Inc., Wallingford CT (2009)
- <sup>21</sup> R. Dennington, T. Keith and J. Millam, GaussView, Version 6, Semichem Inc., Shawnee Mission, KS (2016)
- <sup>22</sup> A. D. Becke, *J. Chem. Phys.*, **98**, 7 (1993), <https://doi.org/10.1063/1.464913>
- <sup>23</sup> C. Lee, W. Yang and R. G. Parr, *Phys. Rev. B*, **37**, 785 (1998), <https://doi.org/10.1103/PhysRevB.37.785>
- <sup>24</sup> A. Jumabaev, H. Hushvaktov, A. Absanov, I. Doroshenko and B. Khudaykulov, *J. Low Temp. Phys.*, **51**, 2 (2025), <https://doi.org/10.1063/10.0035404>
- <sup>25</sup> A. Jumabaev, B. Khudaykulov, U. Holikulov, A. Norkulov, J. Subbiah *et al.*, *Opt. Mater.*, **159**, 116683 (2025), <https://doi.org/10.1016/j.optmat.2025.116683>
- <sup>26</sup> S. Yormatov, U. Holikulov and A. Jumabaev, *Monatsh Chem.*, **157**, 35 (2026), <https://doi.org/10.1007/s00706-025-03402-9>
- <sup>27</sup> A. Jumabaev, S. J. Koyambo-Konzapa and H. Hushvaktov, *J. Mol. Model.*, **30**, 349 (2024), <https://doi.org/10.1007/s00894-024-06147-0>
- <sup>28</sup> U. Sherefedin, A. Belay, K. Gudishe, A. Kebede, A. G. Kumela *et al.*, *Results Phys.*, **68**, 108083 (2025), <https://doi.org/10.1016/j.rinp.2024.108083>

- <sup>29</sup> N. A. B. Beigloo, V. H. Rezvan, G. Ebrahimzadeh-Rajaei and A. Shamel, *J. Mol. Struct.*, **1322**, 140469 (2025), <https://doi.org/10.1016/j.molstruc.2024.140469>
- <sup>30</sup> V. H. Rezvan, *Results Chem.*, **7**, 101437 (2024), <https://doi.org/10.1016/j.rechem.2024.101437>
- <sup>31</sup> B. Khudaykulov, A. Norkulov, U. Holikulov, A. Absanov, I. Doroshenko *et al.*, *J. Low Temp. Phys.*, **51**, 2 (2025), <https://doi.org/10.1063/10.0035406>
- <sup>32</sup> E. Taniş, F. Akman and U. Holikulov, *Russ. J. Phys. Chem. B*, **20**, 150 (2026). <https://doi.org/10.1134/S1990793125701520>
- <sup>33</sup> A. Jumabaev, H. Hushvaktov and A. Absanov, *Bull. Russ. Acad. Sci.: Phys.*, **88**, 1660 (2024), <https://doi.org/10.1134/S106287382470802X>
- <sup>34</sup> N. Sundaraganesan, B. Dominic Joshua, M. Rajamoorthy and C. H. Gangadhar, *Indian J. Pure Appl. Phys.*, **45**, 969 (2007)
- <sup>35</sup> J. Coates, in “Encyclopedia of Analytical Chemistry”, edited by R. A. Meyers, John Wiley & Sons Ltd., 2000, p. 10815
- <sup>36</sup> M. Jeyavijayan and M. Arivazhagan, *Indian J. Pure Appl. Phys.*, **48**, 869 (2010)
- <sup>37</sup> N. R. Babu, S. Subashchandrabose, M. S. A. Padusha, H. Saleem and Y. Erdoğdu, *Spectrochim. Acta A*, **120**, 314 (2013), <https://doi.org/10.1016/j.saa.2013.09.089>